DOE/OR/21400--T480

ornl

C/ORNL 92 0149

OAK RIDGE NATIONAL LABORATORY

MARTIN MARIETTA

CRADA Final Report
for
CRADA Number ORNL92-0149

FRICTION AND WEAR BEHAVIOR OF IN-SITU REINFORCED SILICON NITRIDE

C. S. Yust
Oak Ridge National Laboratory

Dow Chemical

Approved for public release;
distribution is unlimited.

MANAGED BY
MARTIN MARIETTA ENERGY SYSTEMS, INC.
FOR THE UNITED STATES
DEPARTMENT OF ENERGY

C/ORNL--92-0149

MARTIN MARIETTA

MARTIN MARIETTA ENERGY SYSTEMS, INC.

POST OFFICE BOX 2009
OAK RIDGE, TENNESSEE 37831

November 28, 1994

Mr. Peter D. Dayton
Director, Procurement and Contracts
Department of Energy, Oak Ridge Operations
Post Office Box 2001
Oak Ridge, Tennessee 37831-2001

Dear Mr. Dayton:

Final Report for CRADA No. ORNL92-0149 with Dow

The subject CRADA has been completed and enclosed is the Final Report for this project.

This report does not contain proprietary information or Protected CRADA Information. Neither Energy Systems nor the participant object to public distribution of this report.

If you have any questions, please feel free to contact me.

Very truly yours,

C. A. Valentine

for Brian Bovee
Business Manager
Office of Technology Transfer

BBB:cav

Enclosure - As Stated.

cc: File - RC

FINAL REPORT
FOR CRADA
ORNL92-0149

FRICTION AND WEAR BEHAVIOR OF IN-SITU REINFORCED SILICON NITRIDE

C. S. Yust

Metals and Ceramics Division
Oak Ridge National Laboratory
Oak Ridge, TN 37831-6063

Abstract

Specimens of in-situ-reinforced silicon nitride (ISRSN) have been wear tested in lubricated, reciprocating, sliding motion against a silicon nitride counterface. Only mild wear of the ISRSN was observed at contact pressures up to 4.8 GPa at an average sliding velocity of 0.3 m/s. At 0.6 m/s, a wear mode transition was observed in ISRSN at 4.2 - 4.4 GPa. In comparison, the wear mode transition in silicon carbide whisker reinforced silicon nitride at both velocities was evident at about 2.2 - 2.4 GPa. Scanning electron microscopy of the ISRSN wear surfaces revealed the presence of a 40 μm thick debris layer on the mild wear tracks. The ISRSN wear mode transition response indicated a potential for an improved wear resistance in this material as compared to whisker reinforced silicon nitride.

Research sponsored by the U. S. Department of Energy, Assistant Secretary for conservation and Renewable Energy, Office of Transportation Materials, Tribology Program, under Contract AC05-84OR21400 with Martin Marietta Energy Systems, Inc., and by a Cooperative Research and Development Agreement with Dow Chemical Co., Midland, MI.

Introduction

Secondary phases in such forms as particles, platelets, fibersand whiskers, are commonly used to enhance the fracture toughnessof ceramics. As distinct microstructural entities, the second phase features serve to deflect cracks, provide stress fields to interact with those of the propagating crack, and/or bridge the enlarging crack to require the expenditure of additional energy for crack growth beyond that necessary in the monolithic matrix [1,2]. The wear response of several compositions containing whiskers as a reinforcing phase have been investigated in our laboratory, and the results indicated the potential for wear life improvement in some whisker-bearing ceramics [3,4]. Whiskers, however, have been shown to be a possible health hazard because of the ability of small whiskers to become airborne. Consequently, alternate means for whisker-like reinforcement are being investigated, among them the process of in-situ toughening.

In-situ reinforcement refers to the growth of needle-like grains within a microstructure to provide toughening mechanisms similar to that of whiskers. The process is accomplished in silicon nitride by mixing alpha silicon nitride with a sintering aid. At processing temperature, the sintering aid melts and transformation of the alpha phase silicon nitride to beta phase begins. Control of the processing cycle yields a microstructure containing needle-like beta silicon nitride grains within an array of smaller equiaxed grains and a residual intergranular phase. The specifics of the process for the materials investigated in this work are proprietary, in particular the composition of the sintering aid and the process conditions. Both sintering and hot-pressing were used to fabricate dense polycrystalline specimens. This study compared the wear response of the sintered and hot-pressed specimens of in-situ reinforced silicon nitride (ISRSN) with that previously reported for a whisker-reinforced silicon nitride.

Materials and Methods

The materials used in this work were prepared by Dow Chemical Company. The specimens provided were fabricated by two processing techniques, sintering and hot-pressing. Typical properties anticipated for ISRSN are listed in Table I, but these values are not specific to the specimens tested in this work. The fracture toughness of this material, a property of particular significance for wear resistance, is expected to be in the range of 8.5-10 MPa $m^{1/2}$, about twice that of monolithic silicon nitride.

Typical ISRSN microstructures of the sintered and hot-pressed ISRSN materials are shown in Fig. 1. The formation of needle-like grains is evident in both forms, but the presence of an intergranular phase is distinctly shown only in the sintered microstructure. The hot-pressed microstructure appears to be a more porous structure containing a lesser amount of boundary phase material. It is unusual to observe the hot-pressed form of a material to be less dense than the sintered form, and the relatively small amount of grain boundary phase in the hot-pressed body may be a consequence of the polishing process.

The wear test configuration was ball-on-flat, initially using 9.53-mm diameter silicon nitride spheres (NBD 200) as the reciprocating counterface on the ISRSN flats. As testing progressed, it became evident that the contact pressure applied to the interface was limited by the maximum load capacity of the test machine. The use of smaller diameter counterface spheres was adopted to allow higher contact pressures to be attained. Spheres of 6.35 mm and 3.18 mm diameter were used to generate contact pressures as great as 5.2 GPa. Similarly sized spheres of 316 stainless steel were also used as counterface bodies. The surfaces of the test flats, which were approximately 40 mm x 24 mm x 4 mm in size, were ground and polished, finishing with one-half micron diamond paste. The resultant surface roughness of the test surfaces was Ra = 0.02 μm.

The test conditions employed were: a) average sliding velocities of 0.3 m/s and 0.6 m/s; b) applied forces in the range

TABLE I. TYPICAL PROPERTIES OF ISRSN

Flexural Strength at 1370°C	≥490MPa
Stress Rupture 490 MPa @ 100°C	>100hr
Fracture Toughness	>MPam1/2
Weibull Modulus	>18

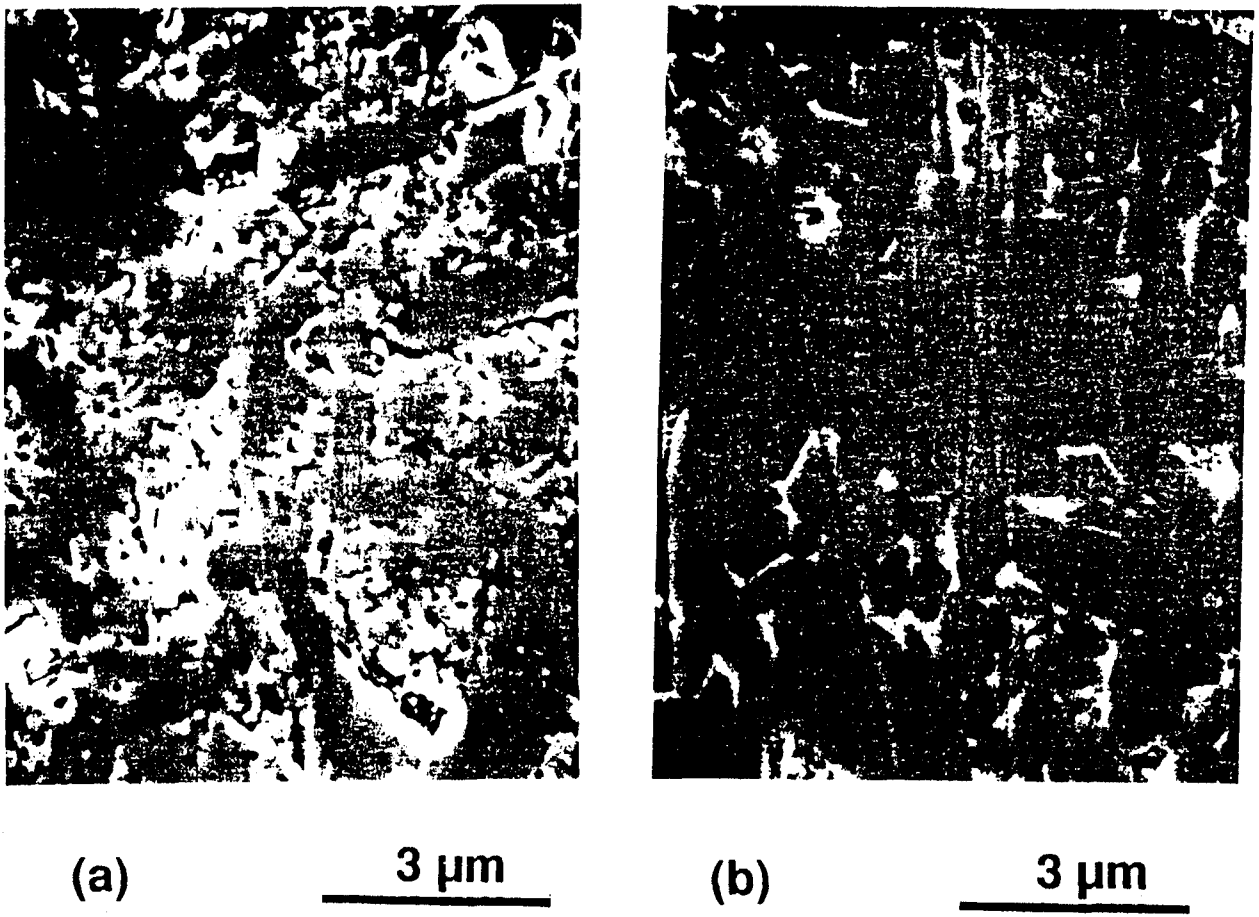

Fig. 1. Scanning electron micrograph of the as-polished surface of (a) hot-pressed ISRSN, and (b) sintered ISRSN. Both forms have elongated, needle-like grains contained within a matrix of equiaxed grains. An intergranular phase is present in the sintered microstructure, but a comparatively small amount of boundary material is observed in the hot-pressed body.

of 50 to 250 N, corresponding to an initial contact pressure range of 2.1 to 5.2 GPa; c) room temperature; d) 50,000 to 300,000 cycles of stress; and e) mineral oil as a lubricant. At the completion of a test, the wear surfaces of both the ball and the flat were examined for evidence of wear. Optical microscopy and scanning electron microscopy were used to examine the wear surfaces. Surface profilometry was used to measure the amount of specimen wear.

Results and Discussion

Friction and Wear

Tests were first performed on both the hot-pressed and sintered material at initial mean Hertzian contact pressures as large as 2.5 GPa at an average velocity of 0.3 m/s and for test durations up to 300,000 cycles of stress. In general, only mild wear was observed on both the pin tip and flat specimen surfaces, although in a few instances, pin tip diameter enlargement, formation of a wear groove, and increased friction coefficient were observed. In subsequent tests using smaller counterface spheres at contact pressures up to 4.8 GPa only mild wear of both pin tip and ISRSN flat were observed. The data summarizing the wear results at 0.3 m/s for both hot pressed and sintered ISRSN specimens are plotted in Fig. 2, as are comparable data for whisker-reinforced silicon nitride (WRSN).

The transition from mild to severe wear is indicated by a marked increase in wear rate and friction coefficient, and is generally accompanied by a significant change in appearance of the wear surface. In ceramics, the formation of large fracture surface areas is characteristic of the wear mode transition. Usually, the wear mode transition is manifest over a small contact pressure increment.

The data presented in Fig. 2 indicate that the wear mode

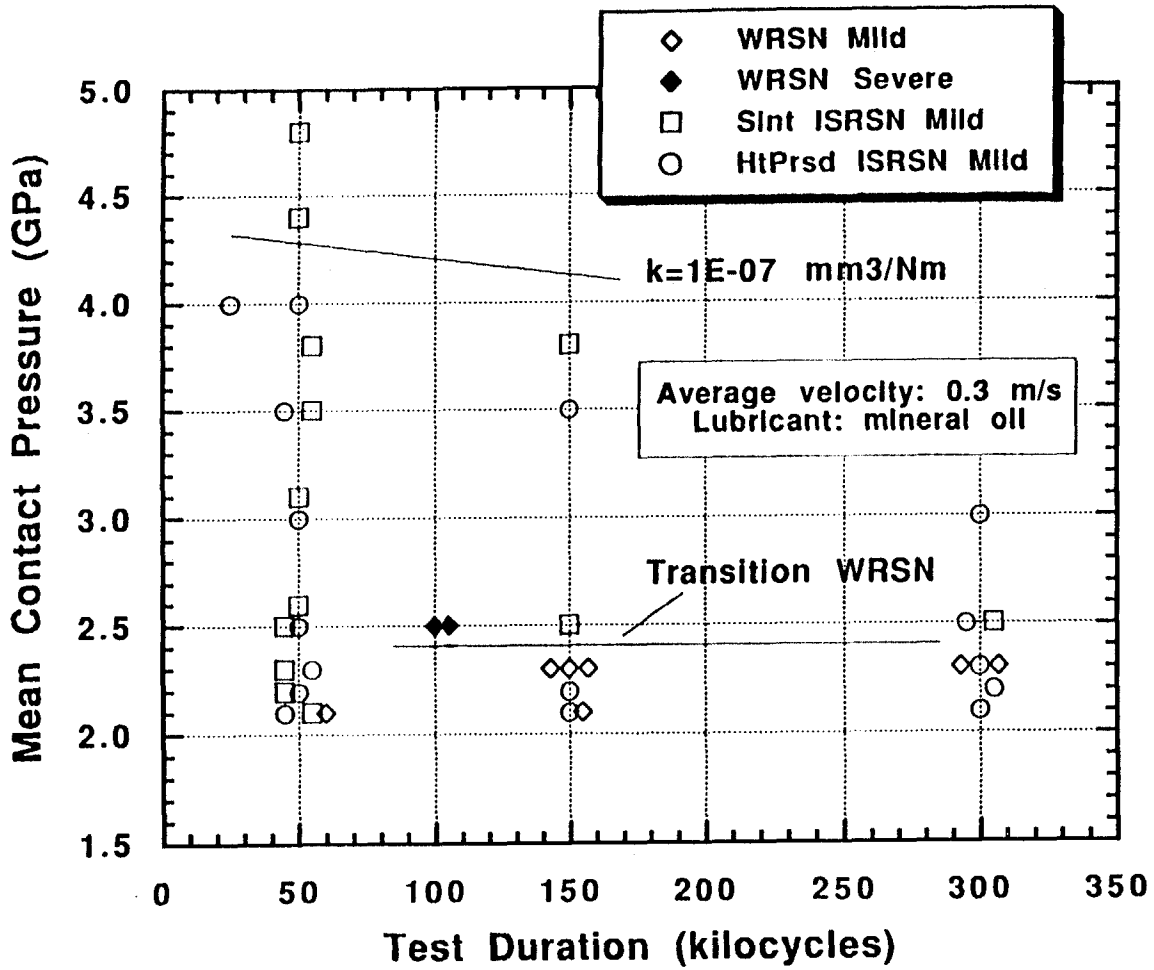

Fig. 2. Accumulated data from tests of ISRSN at an average sliding velocity of 0.3 m/s. A transition is not observed for ISRSN, but an approximate line of constant wear factor is located on the basis of wear factors for the adjacent data points. Wear mode transition data for WRSN from an earlier study are also shown [6].

transition for WRSN takes place at about 2.4 GPa. At 2.3 GPa, mild wear of the composite is observed for test durations to 300,000 cycles. At 2.5 GPa, the transition to severe wear takes place before 100,000 cycles are reached. In contrast, both the hot pressed and sintered forms of ISRSN resist the transition to contact pressures as great as 4.5 to 4.8 GPa. Some increase in the amount of wear is measured as contact pressure is increased, but the characteristics of severe wear, i.e., large dimensional change, extensive debris formation, fracture surface formation, are not observed. The wear factors determined from the wear volumes measured on the worn specimen surfaces are less than 10-6 mm3/N-m, commonly considered to be the limiting wear factor value for mild wear. Based on the wear factor values calculated for the experiments at high contact pressure, an estimated line of constant wear factor of 10-7 mm3/N-m is shown in Fig. 2.

The wear mode transition results at an average sliding velocity of 0.6 m/s are shown in Fig. 3. The wear mode transition was observed in WRSN at a slightly lower contact pressure, 2.2 GPa. A transition was also observed in both forms of ISRSN at this sliding velocity. As the transition lines for the hot-pressed and sintered materials indicate, the data points suggest the possibility of a lower transition contact pressure for the hot pressed microstructure. Approximately twice the contact pressure was required to induce the wear mode transition in mineral-oil lubricated sliding ISRSN than was required for WRSN at 0.6 m/s.

In many of the ISRSN specimens, wear tracks formed by the sliding counterface were not uniform in width or depth, but may contained some localized enlargements. Microscopic examination indicated that these local high-wear regions were frequently associated with microstructural flaws and/or inclusions. Many of the smaller pits formed on the surface also had associated inclusions. These features are discussed in greater detail in the following section. The microstructural discontinuities accompanying the inclusions apparently promote localized increased wear rates, but the extent of wear may be restricted to the vicinity of the inclusion by the in-situ reinforced microstructure.

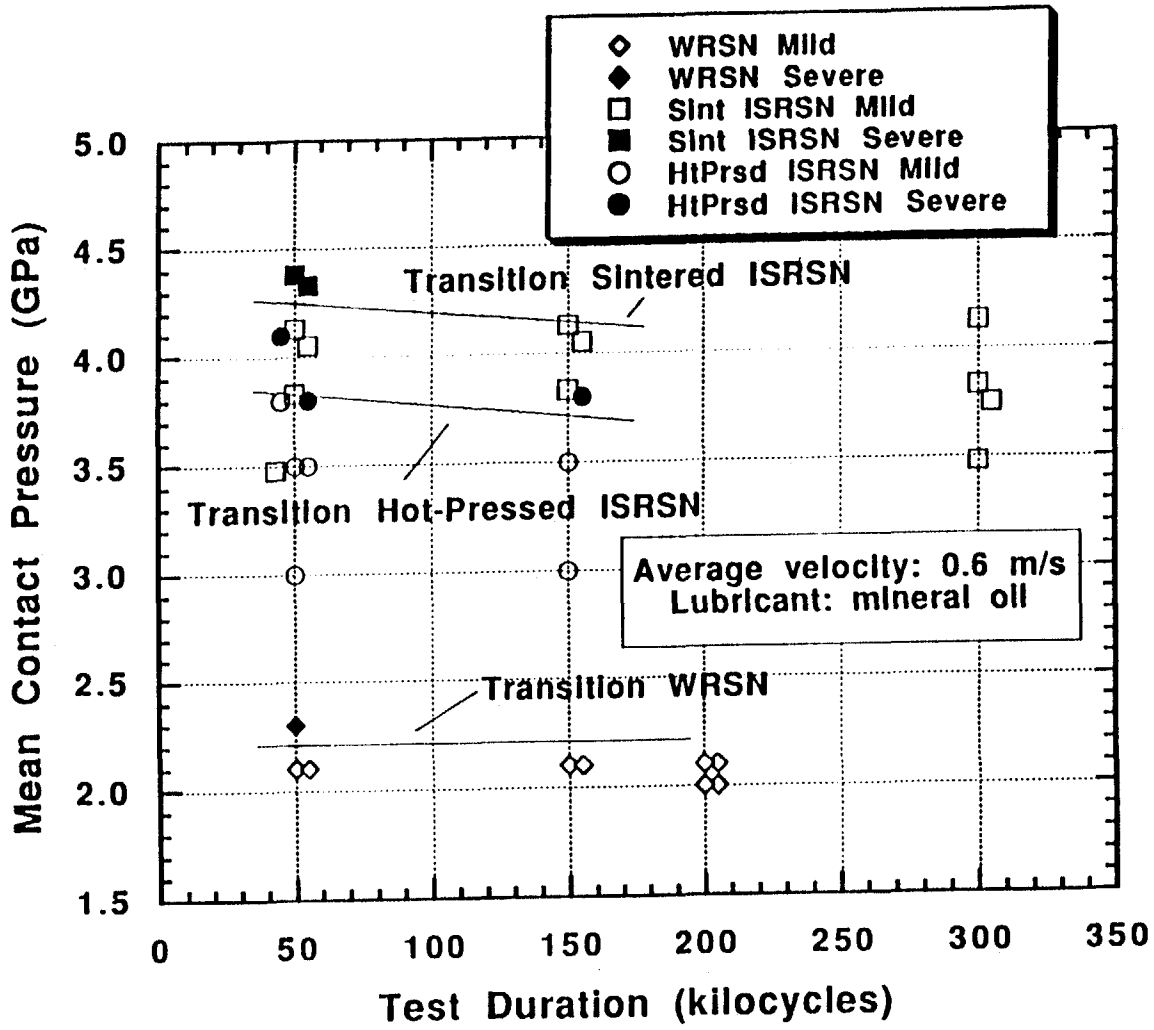

Fig. 3. Accumulated data from tests of ISRSN at an average sliding velocity of 0.6 m/s. A wear mode transition is observed for both hot-pressed and sintered ISRSN. Earlier data for WRSN are shown for comparison [6].

In the case of stainless steel spheres sliding against ISRSN, the results were consistent with those obtained in the sliding of ceramic wear couples. At the lower sliding velocity, 0.3 m/s, the wear track marks were more evident than at 0.6 m/s, although mild wear was indicated in all instances. At the most severe load and velocity conditions applied, some metal adhered to the wear track surface of the sintered ISRSN specimens, less adherence occurring on the hot-pressed ISRSN surface than on the sintered material. Despite the adhered layer of metal (and appearance of near-melting of the steel ball) no significant wear of the ISRSN was observed.

Microscopy

A hot pressed specimen sliding at a contact pressure of 2.5 GPa for a 300,000-cycle test duration (test CP-369) did not exhibit any measurable wear, but the position of the track on the specimen surface was made evident by the accumulation of wear debris from the counterface ball tip. An example of the debris layer formed on the wear path is shown in Fig. 4(a). The debris layer is not completely continuous, containing a distribution of pore-like openings. Additionally, the layer thickness is apparently not uniform, some portions of the layer being lighter in appearance than others. At higher magnification, Fig. 4(b), it is more evident that the layer has varying thickness, the lighter portions being the thicker regions, and the thinner portions transmitting an image of the underlying microstructure. The transmitted underlying image, formed by differential secondary electron emission from grain and boundary phases, indicates the accumulation of debris in the originally empty intergranular spaces of the polished surface (see Fig. 1 (a)). Large pits are not evident on any of the hot-pressed specimen mild wear tracks.

The wear track of the comparable test condition imposed on the sintered material, 2.5 GPa and 300,000 cycles, is shown in Fig. 5. A debris layer similar to that formed on the hot-pressed material was observed. The underlying microstructure is not visible, possibly because the layer is thicker as a result of greater wear

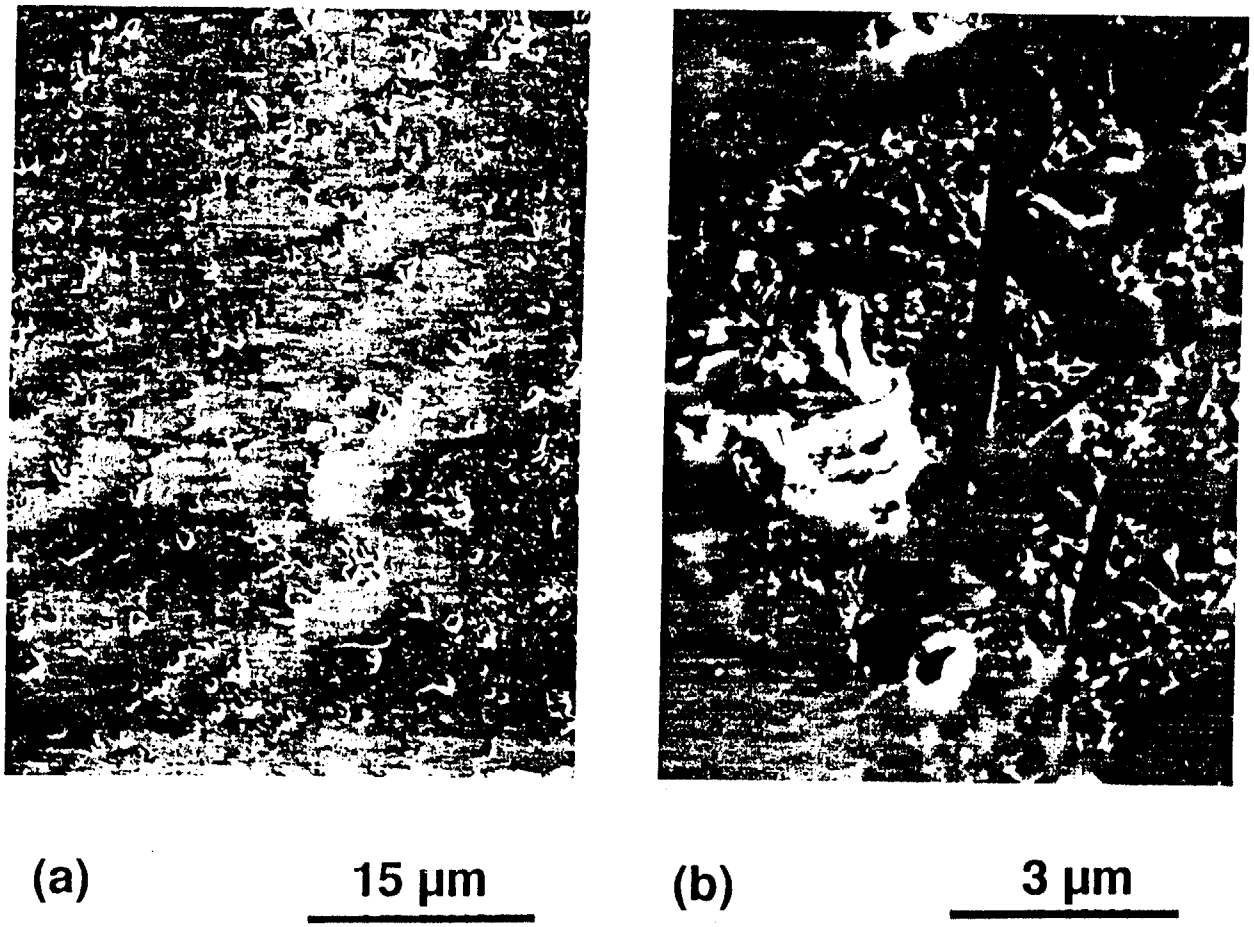

Fig. 4. Scanning electron micrograph of the wear track condition on a hot-pressed specimen after 300,000 cycles at 2.5 GPa contact pressure (test CP-369). As seen in (a), the debris layer contains micrometer-scale openings. At higher magnification, (b), the underlying microstructure is imaged through thin portions of the debris layer.

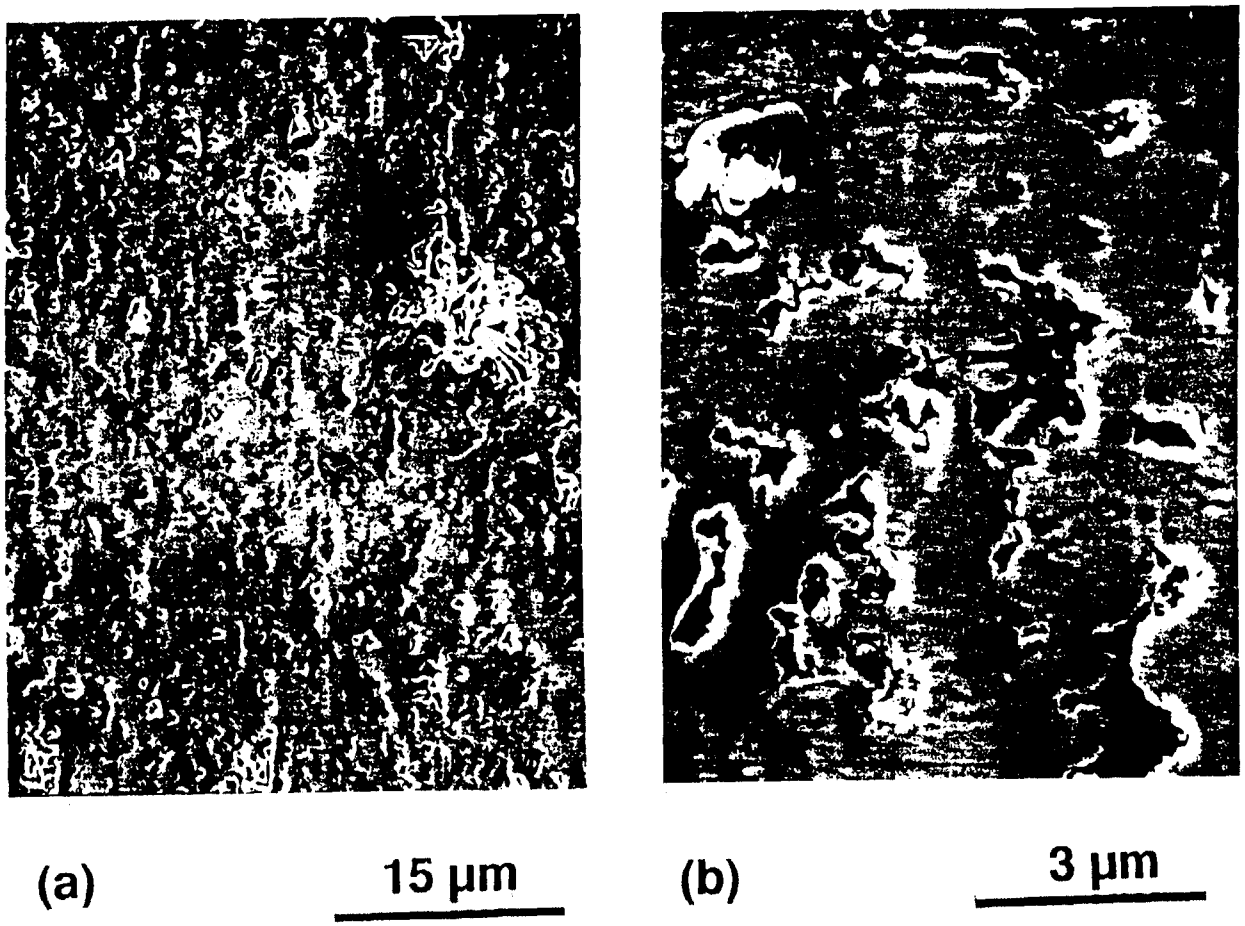

Fig. 5. Scanning electron micrographs of the wear track condition on a sintered specimen after 300,000 cycles at 2.5 GPa contact pressure (test CP-375). The debris layer is similar in appearance to that of the hot-pressed specimen, Fig. 2(a). The underlying microstructure is not imaged, possibly because of a greater layer thickness. Surface shear lines on the debris layer are evident in (b).

Fig. 6. A pit formed in the wear track of a sintered specimen. Fracture started over an area about 7 micrometers in diameter. Extension of the fracture seems to be limited by the needle-like grains.

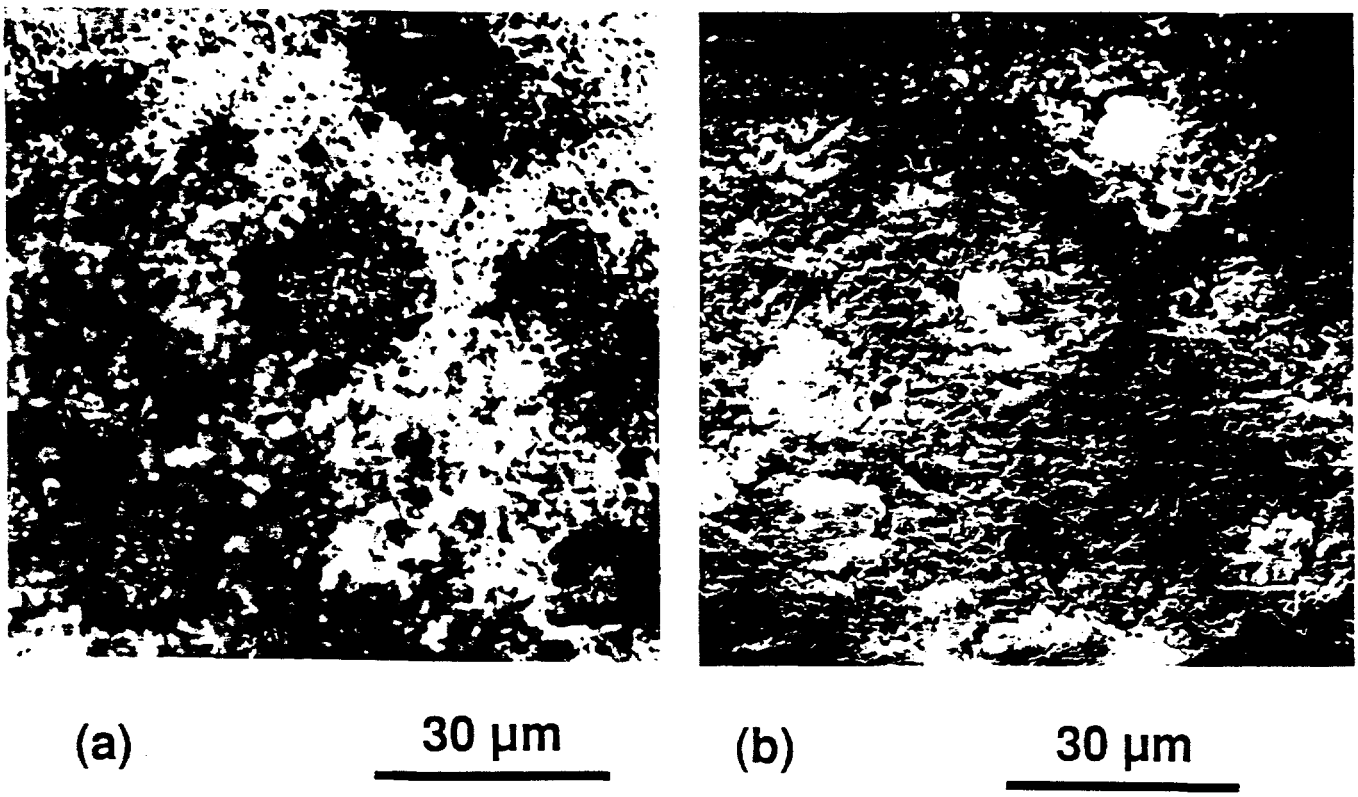

Fig. 7. SEM and optical micrographs of a developing surface pit in sintered ISRSN at 50 kcycles of sliding. The sliding velocity was 0.3 m/s and the contact pressure was 4.4 GPa. The optical microscope view of the inclusions, Fig. 7(a), indicates that they are less reflective than the silicon nitride matrix. The inclusions are detected in the scanning electron microscope image, Fig 7(b), by an increased secondary electron emission.

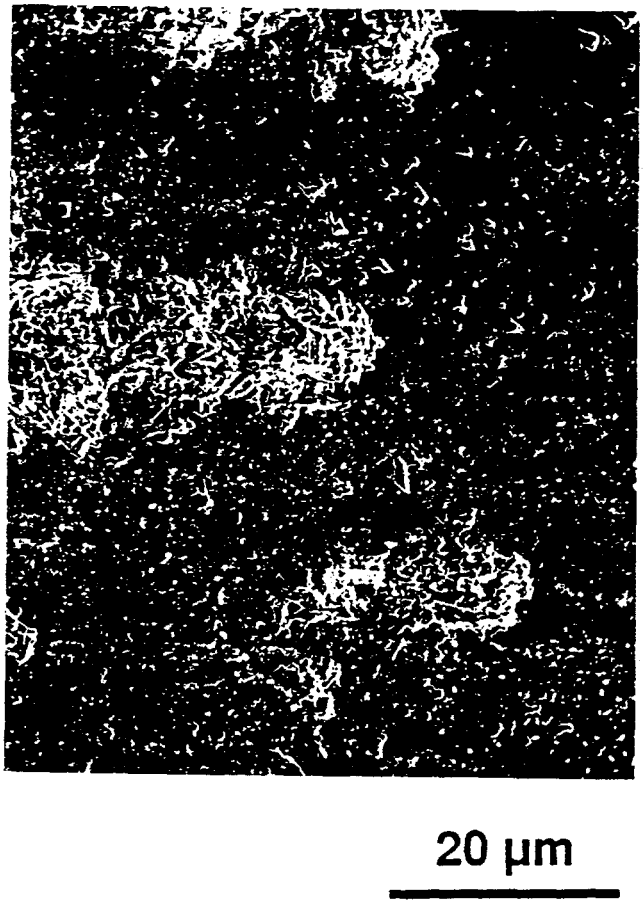

Fig. 8. Pit formation after 150 kcycles of sliding at 0.3 m/s and 3.8 GPa contact pressure. Specimen wear is still in the mild regime, but surface pits are enlarging and increasing in number.

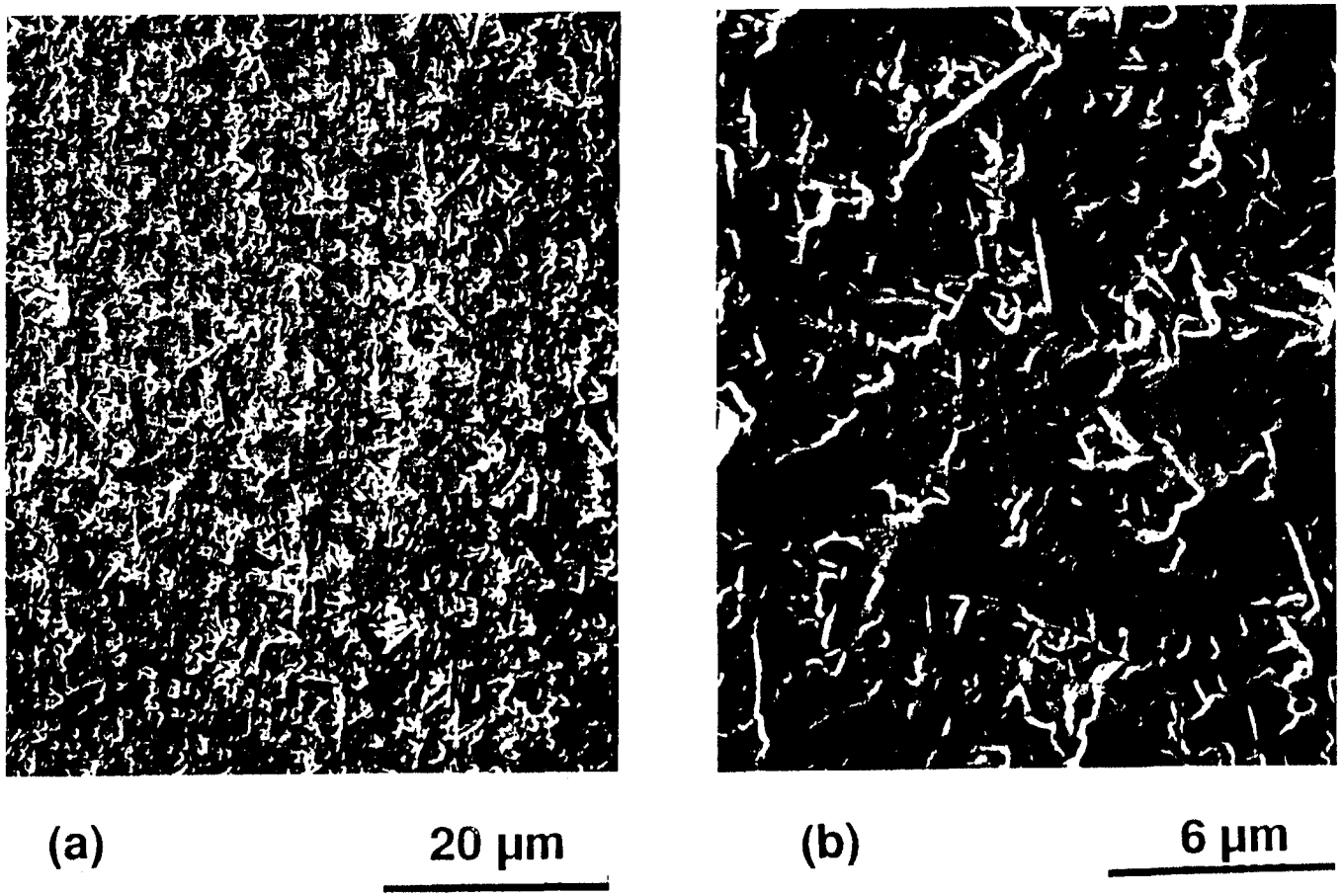

Fig. 9. Surface condition of a sintered specimen after 50 kcycles of sliding at 0.6 m/s at a contact pressure of 4.1 GPa. Wear is not visually evident, and the surface appearance is indistinguishable from the polished condition.

of the counterface ball and compaction of the ball wear debris in the interface. As seen in Fig. 5(b), openings in the debris layer are present similar to those observed on the hot pressed specimen wear surfaces.

On other sintered specimens tested at the same conditions, 2.5 GPa and 300,000 cycles, some pit formation on the wear path was observed by optical microscopy. An SEM view of one such pit showed an area of fracture about 7 microns in diameter, Fig. 6, limited by needle-like grains. The size of the pit was much greater than any residual surface pits on the as-prepared specimen surface, indicating the formation and/or growth of the pit during the wear experiment. The ball tip in this experiment also showed some degree of wear.

At the larger initial contact pressures, greater amounts of wear were observed. While small amounts of material were removed without major disturbance of the surface condition, more substantial material loss in these microstructures appeared to begin with pit formation. For example, at a sliding velocity of 0.3 m/s, and contact pressure of 4.4 GPa, pits of the type shown in Fig. 7 are observed in a sintered specimen surface after 50 kcycles of sliding. Careful examination of these pits, both by optical and electron microscopy, indicated the presence of a more highly reflective phase within a large proportion, although not all, of the pits. The identity of the phase is suggested by the microanalysis results discussed later in this paper.

At a greater test duration, 150 kcycles, at 0.3 m/s and similar contact pressures, the pits were more numerous and deeper, but a complete transition to severe wear had not yet occurred, Fig. 8. Elongated grains of the ISRSN microstructure are visible within the pits.

When the velocity of the silicon nitride ball on the sintered ISRSN surface was increased to 0.6 m/s, pitting was not observed after 50 kcycles of sliding at a contact pressure of 4.1 GPa. The surface appearance of the specimen, Fig. 9, was indistinguishable from that of an unworn polished surface. Material had been removed from the surface, as demonstrated by a profilometer trace of the

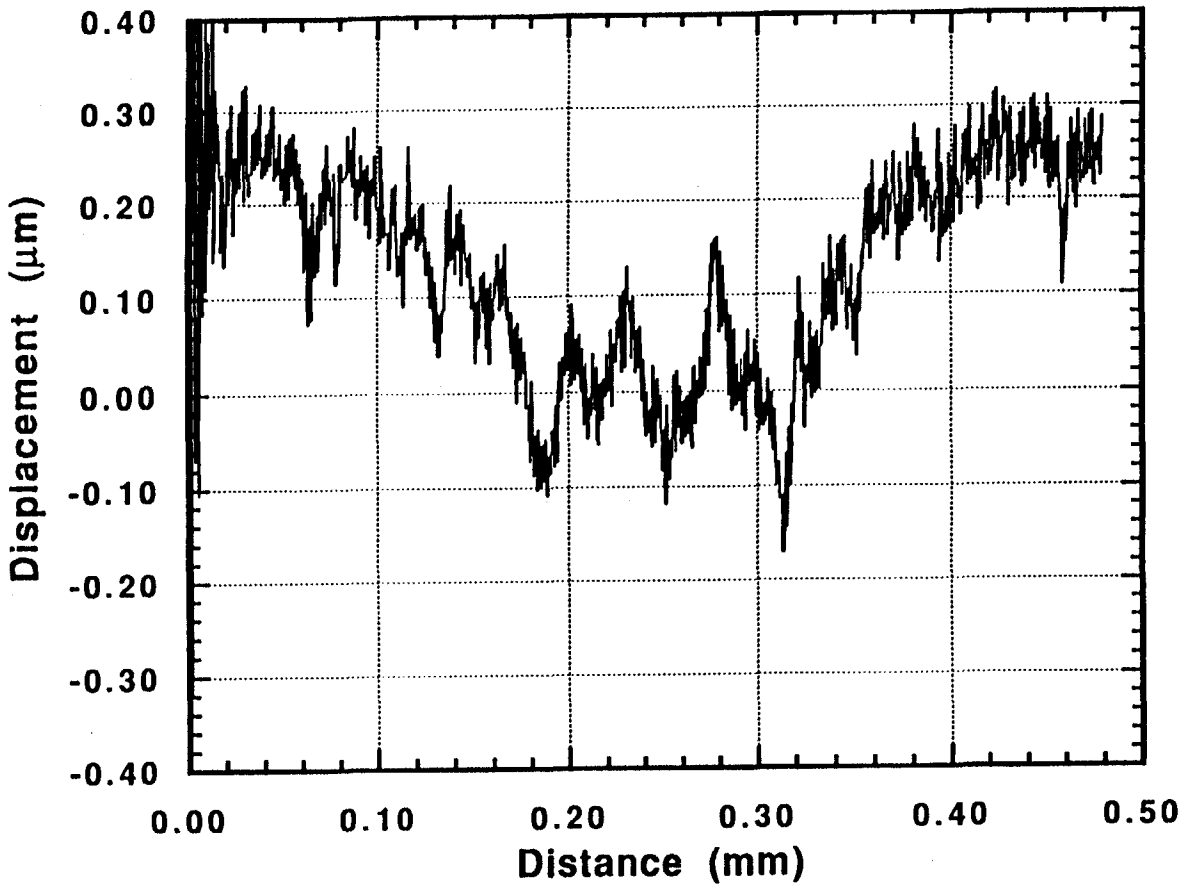

Fig. 10. Profilometer trace of the center of the wear groove shown in Fig. 9. Despite the apparent absence of wear, a groove with an average depth of 0.25 μm has been formed.

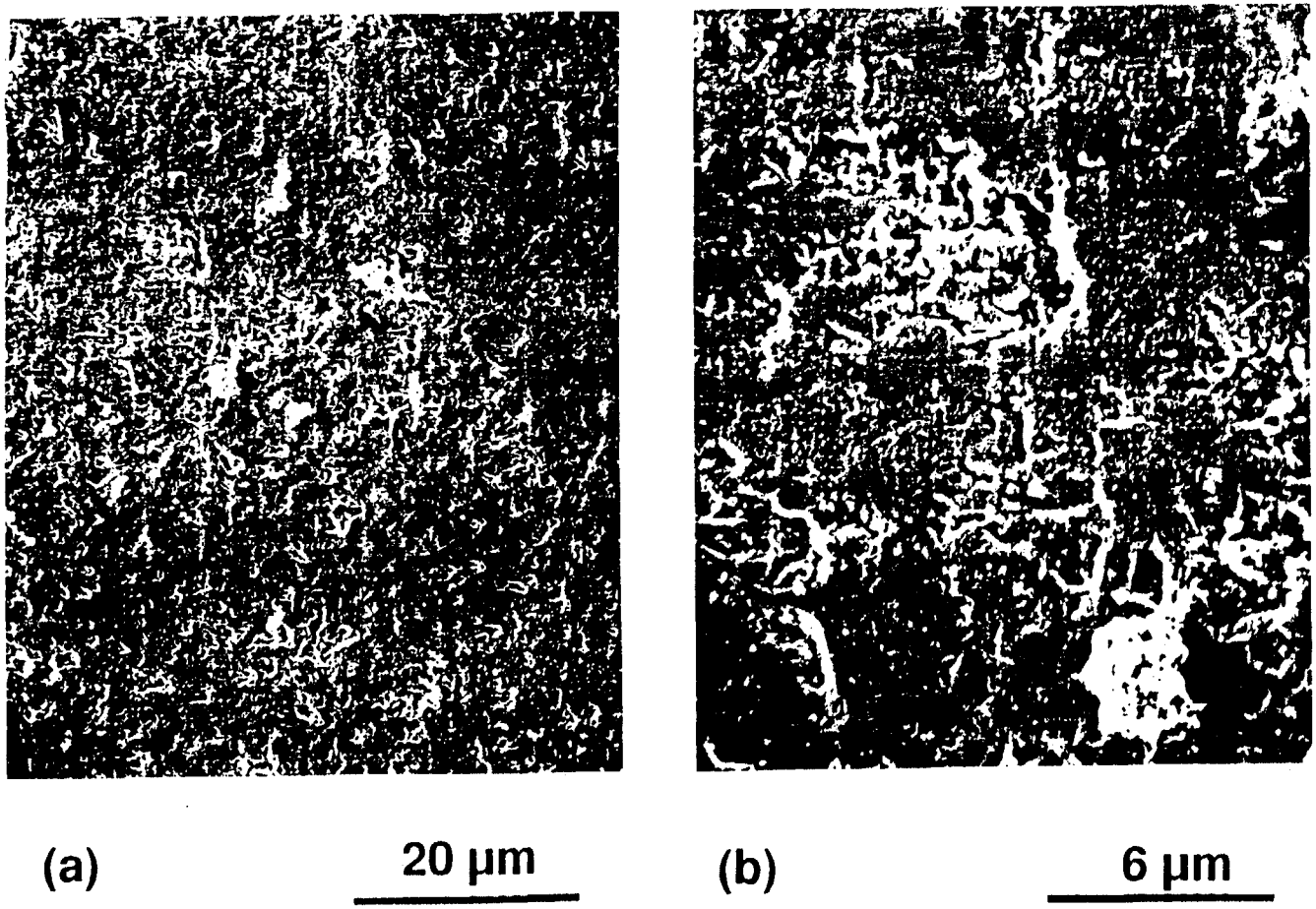

Fig. 11. The wear surface condition in sintered ISRSN after 300 kcycles of sliding at 0.6 m/s at a contact pressure of 4.1 GPa. The wear track surface shows the accumulation of an adhered debris layer and the formation of surface pits.

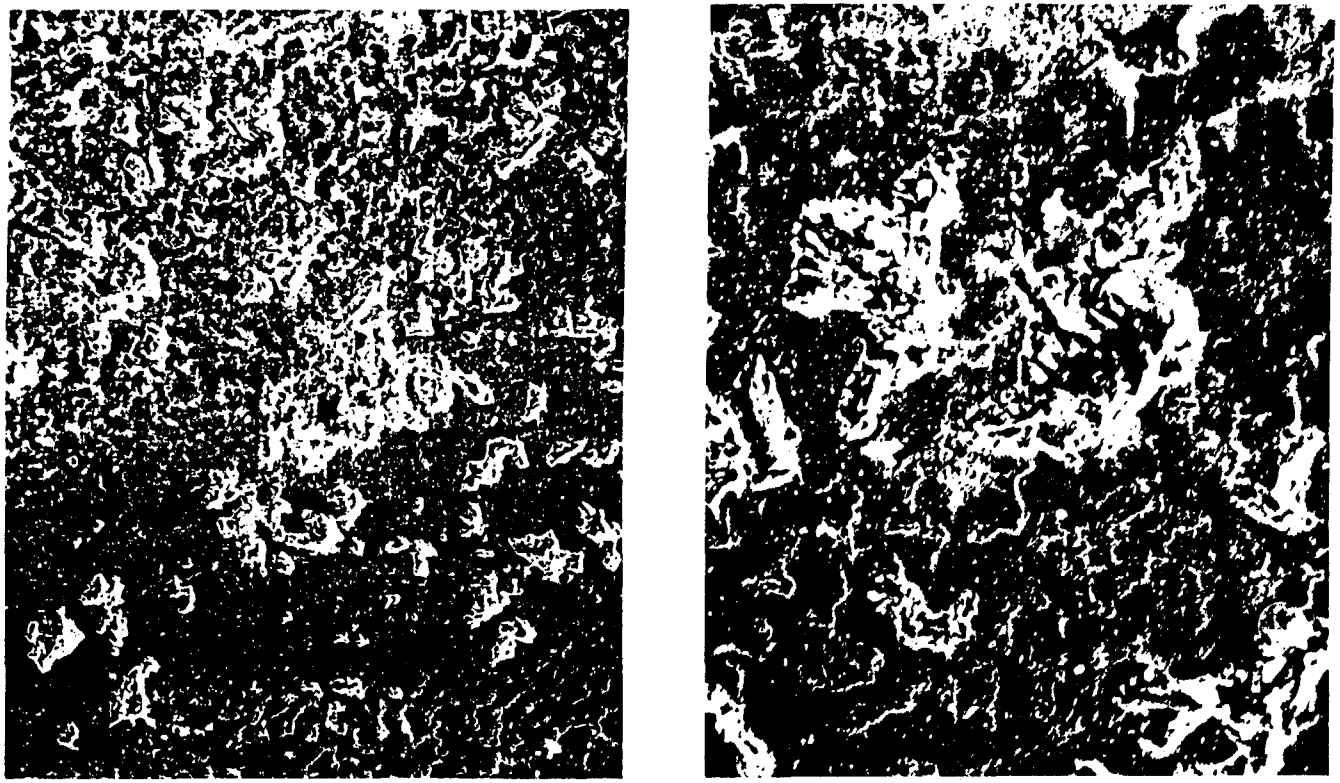

Fig. 12. The wear track condition of a hot-pressed specimen after 50 kcycles of sliding at 0.3 m/s and 4.0 GPa contact pressure. Pitting and formation of an adhered debris layer have started on the wear track.

Fig. 13. At 150 kcycles of sliding at 0.3 m/s, pitting is progressing on the hot-pressed specimen wear track, as indicated by the increase in the number and size of the pits.

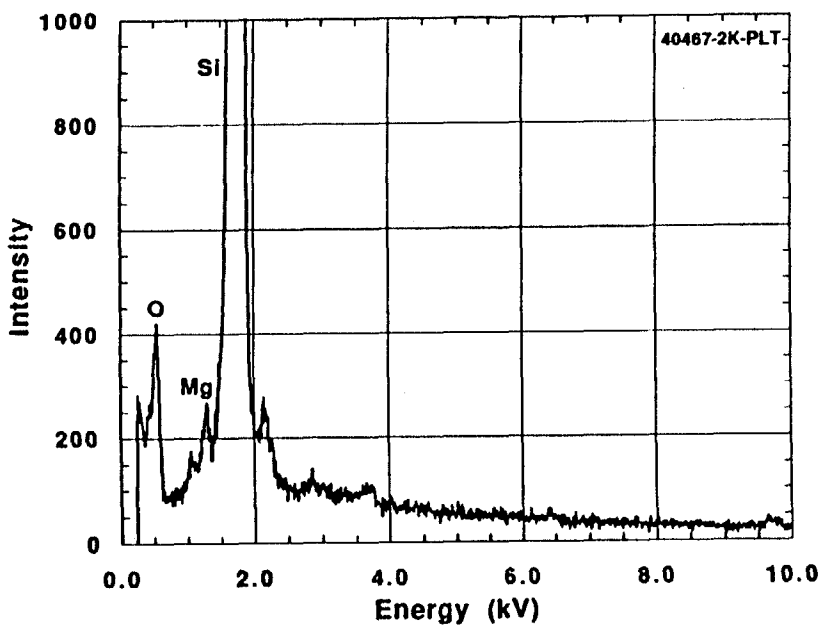

(a)

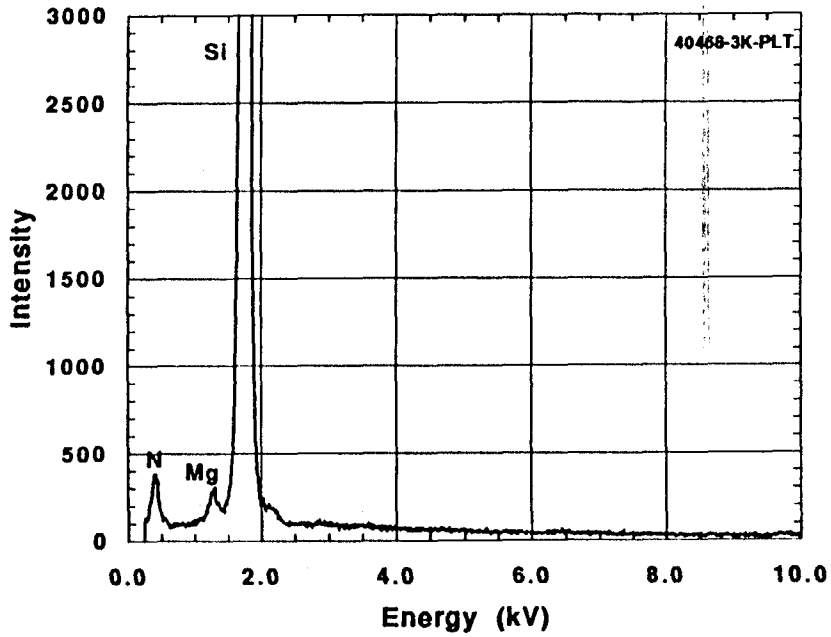

(b)

Fig. 14. (a) X-ray spectrum from the microstructural feature illustrated in Fig. 7. Silicon and oxygen are the principal elements present. (b) the matrix adjacent to the feature is composed primarily of silicon and nitrogen.

center of the groove, Fig. 10. The groove was approximately 0.25 μm deep at the center, and the corresponding wear factor was 5.0 E-09 mm3/N.m, a value consistent with mild wear.

Prolonged sliding of the silicon nitride/sintered ISRSN couple in mineral oil at 0.6 m/s yields the wear surface shown in Fig. 11. A layer of accumulated debris was now evident on the surface, and some pit formation had started, Fig. 11(b). The profilometer trace of this wear track indicated a groove depth of about 0.6 μm, and the wear factor determined for the flat was 1.7E-09 mm3/N.m.

Similar results are obtained when sliding silicon nitride balls on hot-pressed ISRSN. A test duration of 50 kcycles at 0.3 m/s at an initial contact pressure of 4.0 GPa produced a pitted wear track, similar in appearance to that obtained in the sintered material, Fig. 12(a). An adhered debris layer is also formed on the wear track, Fig. 12(b). Fig. 13 shows the progressive enlargement of the surface pits as the sliding duration is extended to 150 kcycles.

Microanalysis of Wear Pits

Two types of microstructural features were observed in many of the wear pits formed on the wear tracks. The proportion of these features in the total pit population was sufficient to suggest that they contribute to pit formation. The main microstructural feature that contributed to pit formation, Fig. 7, was readily distinguished in both optical and SEM photos, respectively, by differences in reflectivity and electron emission. X-ray energy dispersive analysis showed these features were composed primarily of silicon and oxygen, Fig. 14(a). Analysis of the adjacent matrix material revealed only silicon and nitrogen, Fig. 14(b). At the accelerating voltage used during the analysis, the x-rays emitted by oxygen and nitrogen atoms in the material were absorbed to a much greater degree than those from silicon. Despite the disparity in peak heights, the results indicated the presence of a silicon oxide, possibly silica, in these microstructural features. Based upon this result, it is believed that the main microstructural feature is associated with pockets of grain boundary glassy phase.

Note that a small amount of magnesium was also indicated in both results.

The second type of microstrucural feature associated with pit formation, Fig. 15, appeared as a highly reflective feature under optical and SEM analysis. Although relatively few in number, the features have characteristics similar to metallic inclusions. The EDS result indicated the presence of iron, chromium, and nickel, which suggested that the inclusions were a type of stainless steel. Since there were few features of this type, they are expected to have no significant effect on the overall wear behavior.

Wear Transition Surface

Practical utilization of ceramics as machine components requires that the ceramic wear surfaces perform in the mild wear regime throughout the anticipated useful lifetime of the component. The large dimensional changes and debris generation associated with severe wear dictate the restriction of ceramics to mild wear in machine applications. Thus, a critical issue in wear testing is the determination of the conditions at which the wear response begins to undergo a transition from mild to severe wear. The determination of the wear transition surface in a wear space defined by contact pressure, velocity, and stress duration has been described by Yust [5,6]. The tests summarized in this paper are the results of measurements to define that surface for ISRSN.

A comparison of the present results with those obtained for whisker-reinforced silicon nitride is presented as a three-dimensional visualization of the wear surfaces, Fig. 16. The volume of wear space beneath each transition surface corresponds to pressures, velocities, and test durations for which mild wear was observed in each type of material examined. Those conditions above the surface correspond to those for which severe wear would be expected [6]. The transition surface is located at a contact pressure of approximately 2.4 GPa for WRSN at 0.3 m/s, and decreases to about 2.2 GPa at 0.6 m/s. In contrast, the test

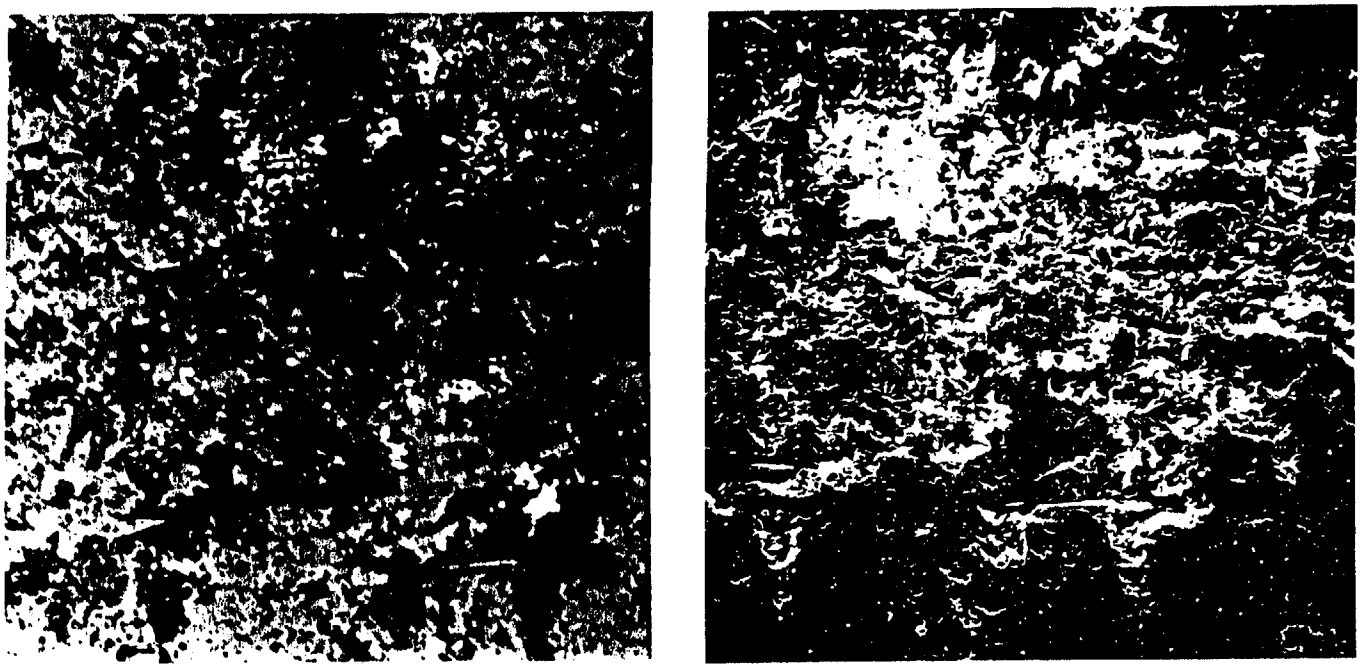

Fig. 15. (a) Photomicrograph of highly reflective microstructural features at the site of a pore in sintered ISRSN. (b) SEM micrograph of the pore shown in (a). Note the greater electron emission from the bright features. EDAX analysis of these features shows that they are composed of iron, chromium, and nickel, suggesting that the material is a stainless steel.

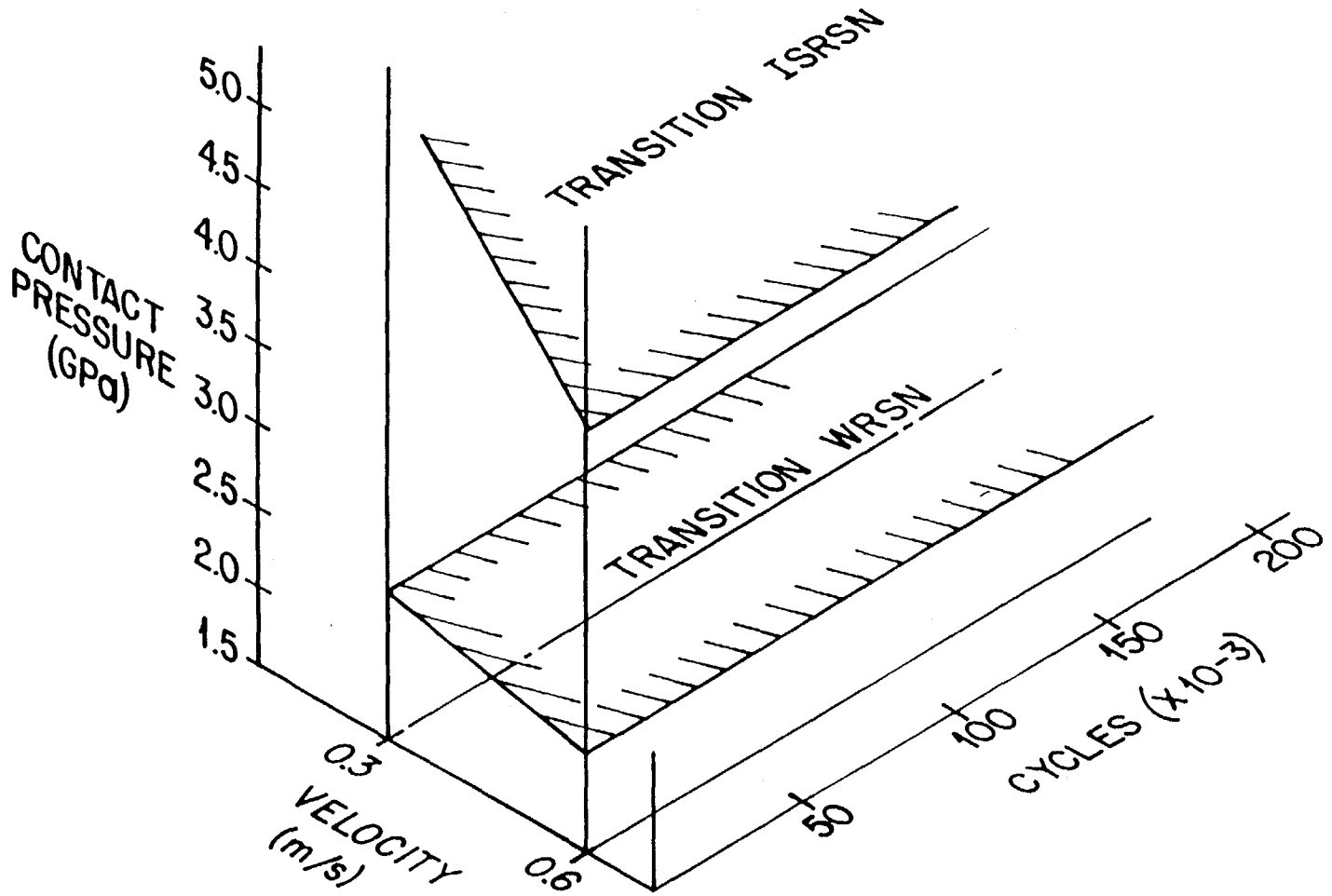

Fig. 16. The wear mode transition diagram for ISRSN and WRSN. The relative positions of the transition surfaces indicate the higher contact pressure required for the mild-to-severe wear mode transition in ISRSN as compared to WRSN.

results reported here for both hot-pressed and sintered ISRSN at contact pressures up to 4.8 GPa at 0.3 m/s showed only mild wear. Accordingly, the wear mode transition surface is depicted as lying somewhat above the 4.8 GPa position at 0.3 m/s. At 0.6 m/s sliding velocity, the observed ISRSN transition contact pressure is approximately 4.2 GPa. The relative positions of the ISRSN and WRSN transition surfaces illustrate the enhanced wear resistance to be expected of ISRSN with respect to WRSN. The magnitude of the contact pressure at which the transition begins in ISRSN in mineral-oil lubricated sliding suggests a potential for effective wear resistance in this material, especially in the presence of formulated lubricants.

Conclusions

1. Mineral-oil lubricated sliding at a velocity of 0.3 m/s on both sintered and hot-pressed ISRSN did not induce a wear mode transition at contact pressures up to 4.8 GPa. Slightly increased wear rates did occur as contact pressure increased, but the associated wear factors did not exceed those characteristic of mild wear. Under comparable conditions, whisker reinforced silicon nitride experienced the wear mode transition at 2.4 GPa. At 0.6 m/s, ISRSN transforms from mild to severe wear at 4.2 - 4.4 GPa, and WRSN transforms at 2.2 GPa.

2. Examination of the ISRSN wear surfaces indicated a greater propensity for pit formation in the sintered material than in the hot-pressed form. Sintered material had the greater retained grain boundary phase, based on observation of the specimen surfaces polished for this study.

3. The test conditions for which the mild-to-severe wear transition was observed in ISRSN were approximately a factor of two greater than those corresponding to the wear mode transition surface for whisker-reinforced silicon nitride. These results

indicate a potential for improved wear resistance in the ISRSN specimens as compared to whisker reinforced silicon nitride.

References

1. Wei, G. C. and Becher, P. F., "Development of SiC-Whisker-Reinforced Ceramics," Ceram. Bull., 64, 2, pp. 298-304 (1985).

2. Becher, P. F. and Tiegs, T. N., "Toughening Behavior Involving Multiple Mechanisms: Whisker Reinforcement and Zirconia Toughening," J. Amer. Ceram. Soc., 79, 19, pp. 651-654 (1987).

3. Yust, C. S. and DeVore, C. E., "Wear of Zirconia-Toughened Alumina and Whisker-Reinforced Zirconia-Toughened Alumina," Trib. Trams. 33, 4, pp. 573-580 (1990).

4. Yust, C. S. and DeVore, C. E., "The Friction and Wear of Lubricated $Si_3N_4/SiC_{(w)}$ Composites," Trib. Trans. 34, 4, pp. 497-504 (1991).

5. Yust, C. S., "Wear Transition Surfaces for Long-Term, Wear Effects," in Tribological Modeling for Mechanical Designers, ASTM STP1105, ASTM, Philadelphia, PA, 1991, pp. 153-161.

6. Yust, C. S., "Wear Mode Transition in a Silicon Nitride-Silicon Carbide Whisker Composite," in Proceedings of the Annual Automotive Technology Development Contractors' Meeting, SAE, Warrendale, PA, 1992, pp. 579-586.

Figure Captions

Fig. 1. Scanning electron micrograph of the as-polished surface of (a) hot-pressed ISRSN, and (b) sintered ISRSN. Both forms have elongated, needle-like grains contained within a matrix of equiaxed grains. An intergranular phase is present in the sintered microstructure, but a comparatively small amount of boundary material is observed in the hot-pressed body.

Fig. 2. Accumulated data from tests of ISRSN at an average sliding velocity of 0.3 m/s. A transition is not observed for ISRSN, but an approximate line of constant wear factor is located on the basis of wear factors for the adjacent data points. Wear mode transition data for WRSN from an earlier study are also shown [6].

Fig. 3. Accumulated data from tests of ISRSN at an average sliding velocity of 0.6 m/s. A wear mode transition is observed for both hot-pressed and sintered ISRSN. Earlier data for WRSN are shown for comparison [6].

Fig. 4. Scanning electron micrograph of the wear track condition on a hot-pressed specimen after 300,000 cycles at 2.5 GPa contact pressure (test CP-369). As seen in (a), the debris layer contains micrometer-scale openings. At higher magnification, (b), the underlying microstructure is imaged through thin portions of the debris layer.

Fig. 5. Scanning electron micrographs of the wear track condition on a sintered specimen after 300,000 cycles at 2.5 GPa contact pressure (test CP-375). The debris layer is similar in appearance to that of the hot-pressed specimen, Fig. 2(a). The underlying microstructure is not imaged, possibly because of a greater layer thickness. Surface shear lines on the debris layer are evident in (b).

Fig. 6. A pit formed in the wear track of a sintered specimen.

Fracture started over an area about 7 micrometers in diameter. Extension of the fracture seems to be limited by the needle-like grains.

Fig. 7. SEM and optical micrographs of a developing surface pit in sintered ISRSN at 50 kcycles of sliding. The sliding velocity was 0.3 m/s and the contact pressure was 4.4 GPa. The optical microscope view of the features within the pit, Fig. 7(a), indicates that they are less reflective than the silicon nitride matrix. The features are detected in the scanning electron microscope image, Fig 7(b), by an increased secondary electron emission.

Fig. 8. Pit formation after 150 kcycles of sliding at 0.3 m/s and 3.8 GPa contact pressure. Specimen wear is still in the mild regime, but surface pits are enlarging and increasing in number.

Fig. 9. Surface condition of a sintered specimen after 50 kcycles of sliding at 0.6 m/s at a contact pressure of 4.1 GPa. Wear is not visually evident, and the surface appearance is indistinguishable from the polished condition.

Fig. 10. Profilometer trace of the center of the wear groove shown in Fig. 9. Despite the apparent absence of wear, a groove with an average depth of 0.25 μm has been formed.

Fig. 11. The wear surface condition in sintered ISRSN after 300 kcycles of sliding at 0.6 m/s at a contact pressure of 4.1 GPa. The wear track surface shows the accumulation of an adhered debris layer and the formation of surface pits.

Fig. 12. The wear track condition of a hot-pressed specimen after 50 kcycles of sliding at 0.3 m/s and 4.0 GPa contact pressure. Pitting and formation of an adhered debris layer have started on the wear track.

Fig. 13. At 150 kcycles of sliding at 0.3 m/s, pitting is progressing on the hot-pressed specimen wear track, as indicated by the increase in the number and size of the pits.

Fig. 14. (a) X-ray spectrum from the microstructural feature illustrated in Fig. 7. Silicon and oxygen are the principal elements present. (b) the matrix adjacent to the feature is composed primarily of silicon and nitrogen.

Fig. 15. (a) Photomicrograph of highly reflective microstructural features at the site of a pore in sintered ISRSN. (b) SEM micrograph of the pore shown in (a). Note the greater electron emission from the bright features. EDAX analysis of these features shows that they are composed of iron, chromium, and nickel, suggesting that the material is a stainless steel.

Fig. 16. The wear mode transition diagram for ISRSN and WRSN. The relative positions of the transition surfaces indicate the higher contact pressure required for the mild-to-severe wear mode transition in ISRSN as compared to WRSN.